Article

Binding Affinity of Trastuzumab and Pertuzumab Monoclonal Antibodies to Extracellular HER2 Domain

Victor L. Cruz, [1]* Virginia Souza-Egipsy, [1] María Gion, [2] José Pérez-García, [3,4] Javier Cortes, [3,4,5] Javier Ramos [1] and Juan F. Vega [1]

[1] BIOPHYM, Department of Macromolecular Physics, Instituto de Estructura de la Materia, IEM-CSIC, C/Serrano 113 bis, 28006 Madrid, Spain
[2] University Hospital Ramon y Cajal, Madrid (Spain)
[3] International Breast Cancer Center (IBCC), Pangaea Oncology, Quironsalud Group, Barcelona (Spain)
[4] Medical Scientia Innovation Research (MedSIR), Barcelona (Spain)
[5] Faculty of Biomedical and Health Sciences, Department of Medicine, Universidad Europea de Madrid, Madrid (Spain)
* Correspondence: author: vl.cruz@csic.es

This paper is dedicated to the memory of our dear colleague Prof. J. Martínez-Salazar.

Abstract: The binding affinity of trastuzumab and pertuzumab to HER2 has been studied using both experimental and in-silico methods. The experiments were conducted using the antibodies in their complete IgG form, as used in clinical therapy, and the extracellular domain of the HER2 protein in solution. This approach provides a precise, reproducible, and reliable view of the interaction between them in physiological conditions. Dynamic light scattering and size exclusion chromatography coupled with tetra detection were utilized to characterize the protein complexes, measure their concentrations, and calculate the equilibrium free binding energy, ΔG_{bind}. In addition, PRODIGY, a QSAR-like model with excellent predictive ability, was employed to obtain in-silico ΔG_{bind} estimations. The results obtained indicate that pertuzumab exhibits a slightly higher binding affinity to HER2 than trastuzumab. The difference in binding affinity was explained based on the contribution of the different interfacial contact (IC) descriptors to the ΔG_{bind} value estimated by the PRODIGY model. Furthermore, experiments revealed that the pertuzumab IgG antibody binds preferentially to two HER2 proteins, one per Fab fragment, while trastuzumab mainly forms a monovalent complex. This finding was interpreted based on a geometrical model that identified steric crowding in the trastuzumab-HER2 complex as compared to the pertuzumab-HER2 complex.

Keywords: Trastuzumab; Pertuzumab; HER2; Binding Free Energy; PRODIGY; Size Exclusion Chromatography

1. Introduction

Monoclonal antibodies (mAbs) have emerged as highly effective and successful anticancer therapies. In particular, the human epidermal growth factor receptor 2 (HER2) is a widely recognized antigen targeted by various antibodies for the treatment of HER2 overexpressed cancers [1]. Trastuzumab is the most frequently used mAb against HER2, specifically targeting the extracellular domain IV of the receptor [2]. Pertuzumab, another anti-HER2 mAb, binds to domain II, the dimerization arm of HER2 [3].

Several experimental studies have analyzed the binding affinity of each antibody to HER2. Troise et al. investigated the binding between HER2 and trastuzumab using three different methods (ELISA, SPR, ITC) at room temperature. They estimated the free energy of binding (ΔG_{bind}) to be -11.0 ± 3.0 kcal·mol^{-1} [4]. In another study, Lua et al. conducted a binding kinetics analysis of the interaction between the extracellular domain of HER2 and both antibodies, alone or in sequential combination, by using a BLItz biosensor technology. The estimated ΔG_{bind} values were -11.1 and -10.5 kcal·mol^{-1} for trastuzumab and pertuzumab antibodies, respectively. In addition, they explored both the whole

 doi:10.20944/preprints202306.0676.v1

antibody and only its Fab subdomain. They observed a slightly preferential binding for trastuzumab over pertuzumab in both antibody forms, namely, Fab or complete IgG form [5]. Furthermore, Spiegelberg et al. determined dissociation constants for HER2/trastuzumab and HER2/pertuzumab complexes using the ligand tracer technique on living cell lines [6]. Their study revealed ΔG_{bind} values of -13.7 and -14.0 kcal·mol^{-1} for the trastuzumab and pertuzumab complexes at 310 K, respectively.

The molecular structures of the complexes formed by the HER2 extracellular domain and the Fabs of the trastuzumab and pertuzumab antibodies have been investigated using crystallography techniques [2,3]. In addition, cryoelectron microscopy has been employed to examine ternary complexes involving the HER2 antigen with both trastuzumab and pertuzumab Fabs [7]. The availability of such detailed structural information has facilitated several "in-silico" studies in these systems. Fuentes et al. performed MD simulations and MMPBSA calculations to estimate the $\Delta G_{bind,}$ [8]. and their results indicated that trastuzumab exhibits stronger binding affinity compared to pertuzumab. They also suggested the presence of a potential synergistic effect between the two antibodies based on their mutual interaction. Nonetheless, the large size of the protein complexes posed a significant limitation for the simulation models used due to inadequate sampling.

In this study, we have conducted a biophysical analysis to investigate the binding characteristics of pertuzumab and trastuzumab antibodies in their interaction with the extracellular HER2 domain. In contrast to previous studies, we have employed a label-free method to quantitative characterize macromolecular interactions under physiological conditions. To the best of our knowledge, this methodology has not yet been tested for this case. Specifically, we employed Size Exclusion Chromatography (SEC) to examine the binding process of each monoclonal antibody to HER2. In our previous studies, SEC has been successfully applied to analyze the hydrodynamic properties of aqueous solutions containing extracellular HER2 domain, trastuzumab, and their complexes [9]. It is noteworthy that the experimental design in this study was based on a solution-phase approach that considered the entire IgG antibody as it is used in clinical therapy. This approach is known to yield more realistic results compared to protocols that rely on chip antibody immobilization techniques [10].

Our in-silico approach begins with the crystallographic structures to provide atomistic details of the intermolecular interactions between the antibodies and the antigen. Specifically, we have adopted the protein-protein binding model proposed by Vangone et al. [11]. to analyze each type of interaction and its individual contribution to the overall binding affinity. This quantitative structure activity relationship (QSAR) model correlates with structural descriptors of the protein complexes that specifically pertain to their interaction within the binding region. To create the model, the authors have used a curated database of experimental data on protein complexes for which crystallographic resolved structures were available, resulting in correlations with excellent predictive performance.

Other added value of this approach is its ability to provide a straightforward interpretation of the structural descriptors that contribute to the model, including residue-residue interaction types (e.g., charged-charged, charged-polar, polar-apolar, …) and non-interacting molecular surfaces. It is worth noting that we opted against using molecular simulation approaches to calculate ΔG_{bind}, given the large size of the systems. Such simulations would require significant computational resources to achieve adequate sampling and converged values.

2. Materials and Methods

2.1. Experimental details

2.1.1. Samples

The mAbs pertuzumab Perjeta© and trastuzumab Herceptin© (stock solution at 30 and 21 mg·mL^{-1}, respectively) were kindly provided by one of us (JC) from Hospital Ramón y Cajal (Madrid, Spain). The glycosylated HER2 receptor ectodomain tagged with a 10-length polyhistidine peptide on the C-terminal (g-eHER2) was purchased from Sino Biological, Inc. (Beijing, China). Desalting and

Preprints (www.preprints.org) | NOT PEER-REVIEWED | Posted: 9 June 2023 doi:10.20944/preprints202306.0676.v1

buffer exchange have been carried out with centrifugal concentrators (Amicon Ultra-0.5 mL, Merck Millipore, Billerica, MA, USA). All solutions were filtered (Millex-GV 0.22 μm, Merck Millipore, Billerica, MA, USA) and stored in 20 mM Tris-HCl pH 7.5, 150 mM NaCl to subsequent analysis and to prepare g-eHER2/mAbs mixtures at the selected molar ratio 1:3. Water for all buffers and dilution was obtained from Milli-Q water purification system (Merck Millipore, Billerica, MA, USA). The initial concentrations of g-eHER2 and mAbs were 0.3 and 1.0 mg·mL^{-1}, respectively. Total initial concentration of protein in the mixtures has been maintained nearly constant, around 0.85 - 0.90 mg·mL^{-1}. Solutions were mixed at 300 r.p.m. and T = 309 K during 30 minutes in an Eppendorf Thermomixer (Eppendorf, Enfield, CT, USA).

2.1.2. Basic hydrodynamic characterization of e-HER2 receptor and mAbs

Dynamic light scattering (DLS) electric field correlations have been obtained for the g-eHER2 and mAbs solutions prepared as indicates above, using the Zetasizer Nano ZS (Malvern Instruments, Worcestershire, UK) at T = 309 K, equipped with disposable cuvettes (Malvern Instruments ZEN0040). The readers are referred to previous publications for the experimental details [9,12]. This technique allowed us to extract the diffusion coefficient, D_s, from the autocorrelation function. Hydrodynamic size, r_h, has been obtained from the results obtained for D_s, the diffusion coefficient at infinite dilution, using the Stokes-Einstein equation:

$$D_s = \frac{k_B T}{6\pi\eta r_h} \quad (1)$$

with k_B, the Boltzmann constant and η the buffer viscosity at T = 309 K. The results obtained for D_s and r_h are shown in Table 1.

Molecular weight and concentration of g-eHER2 receptor, mAbs and complexes

The determination of the molecular weight, M_w, and the concentration of the g-eHER2 receptor, the mAbs, and the HER2/mAbs complexes in solution was carried out by means of size exclusion chromatography (SEC) coupled with tretradetection using the GPCmax-TDA system (Malvern Instruments, Worcestershire, UK) at T = 309 K. A GE Superose™ 300 column (GE Healthcare, Buckinghamshire, UK) was equilibrated with a buffer composed of 20 mM Tris pH 7.5, 150 mM NaCl. 100 μL of sample at a total concentration of c ~ 0.80 - 0.85 mg·mL^{-1} were injected into the SEC column and eluted with the equilibration buffer at a flow rate of 0.5 mL·min^{-1} (see Table 1). Elution profiles were followed by a UV-photo diode array (UV-PDA), a differential refractometer (RI), a 7° low angle light scattering detector (LALS) and a 90° right angle light scattering detector (RALS). Bovine serum albumin (BSA) was used as standard reference protein of known molecular weight, concentration and refractive index increment (dn/dc = 0.185 mL·g^{-1}). The OmniSEC software program was used for the data acquisition and analysis, including the absolute molecular weight, M_w, the intrinsic viscosity, [η], the specific absorption coefficient, dA/dc (Table 1), and finally the concentration, c, of each sample were determined (Table 2).

2.2. In-silico Methods

2.2.1. Molecular Dynamics Simulations

The starting structures for the extracellular HER2 domain and the Fabs of the mAbs trastuzumab and pertuzumab were extracted from the protein data bank (codes:1N8Z for the HER2/trastuzumab[2] Fab complex and 1S78 for the HER2/pertuzumab[3] Fab complex). Missing residues in both structures were filled using the protein loop tools available in the Discovery Studio package [13]. The Molecular Mechanics models selected for the simulation consist of the force field ff14SB [14]. for proteins as implemented in the Amber 16 suite of programs [15]. This model contains the adequate parameters for the systems considered in this work. The models built for each protein complex described in the previous point were subjected to the same refinement protocol described in previous works [9,12].

Preprints (www.preprints.org) | NOT PEER-REVIEWED | Posted: 9 June 2023 doi:10.20944/preprints202306.0676.v1

2.2.2. PRODIGY QSAR Model

A subset of 20 snapshots at 1ns interval corresponding to the final 20 ns of the NVT simulations for each system was submitted to the PRODIGY webserver for binding energy evaluation [16]. The QSAR equation used to evaluate binding affinity was that described by Vangone et al.:

$$\Delta G_{predicted} = -0.09459\, IC_{\frac{charged}{charged}} - 0.10007\, IC_{\frac{charged}{apolar}} + 0.19577\, IC_{\frac{polar}{polar}} -$$

$$0.22671\, IC_{\frac{polar}{apolar}} + 0.18681\, \%NIS_{apolar} + 0.3810\%NIS_{charged} - 15.9433 \qquad (2)$$

where ICs corresponds to nature-dependent antigen-antibody interfacial contacts and NIS is the percentage of non-interacting surface (see ref. [17]. for details). Two residues are defined in contact if any of their heavy atom is within a distance of 5.5 Å. The final ΔG values were averaged over the results obtained for each structural set submitted to the PRODIGY webserver. The IC descriptor is the number of contacts between residues of the interacting proteins according to the aminoacid types. The aminoacids are classified as: charged (E, D, K, R), polar (C, H, N, Q, S, T, W) and apolar (A, F, G, I, L, V, M, P, Y). The subscript in each of these IC descriptors shown in equation (2) refers to the residue classes of the interacting proteins. For example, $IC_{\frac{charged}{apolar}}$ is the number of contacts between charged residues of one protein and apolar residues of the other.

3. Results

3.1. Experimental findings

The SEC profiles of the samples at c ~ 0.3 mg·mL^{-1} (for g-eHER2) and c ~ 1.0 mg·mL^{-1} (for mAbs), obtained from the different detectors is envisaged in Figure 1 (up).

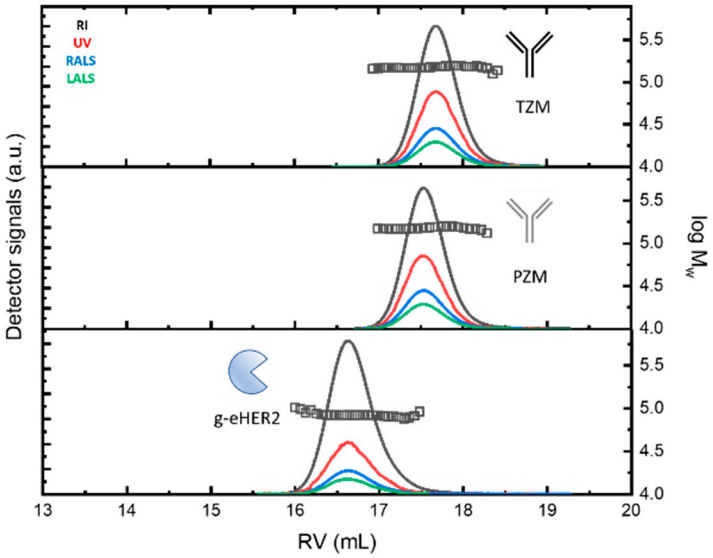

Preprints (www.preprints.org) | NOT PEER-REVIEWED | Posted: 9 June 2023 doi:10.20944/preprints202306.0676.v1

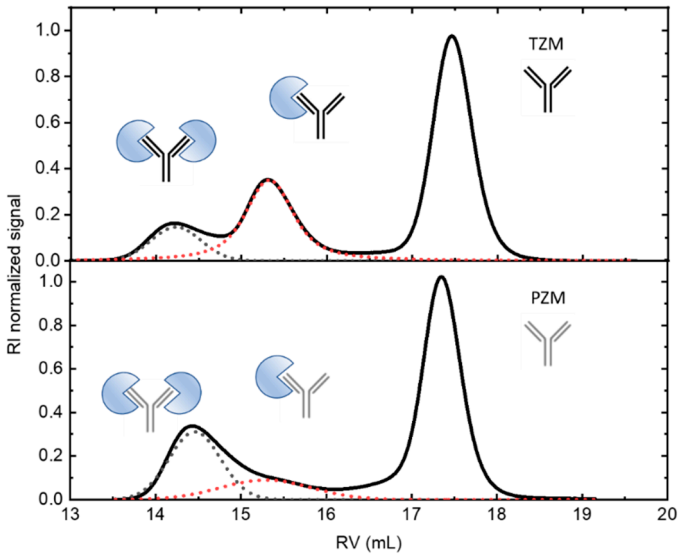

Figure 1. (Up) SEC/tetradetection profiles of the mAbs, trastuzumab (TZM) and pertuzumab (PZM), and the antigen, g-eHER2. The lines represent the profiles obtained from the different detectors. The symbols represent the measured absolute molecular masses. (**Down**) SEC/tetradetection profiles of g-eHER2/TZM and g-eHER2/PZM mixtures. The dashed lines represent the deconvolution of complex 1 and 2 signals to determine the corresponding concentrations.

Both mAbs show a similar profile at around a retention volume of 17.5 - 17.6 mL. Absolute molecular masses of 146.0 - 147.0 kDa were measured (symbols). The observed molecular mass values agree with the typical molecular size for antibodies of the IgG type (see Table 1). The differences found among the values taken after 5 independent measurements are lower than 2 %. g-eHER2 elutes around 16.6 mL, having a measured absolute molecular mass of 86.4 kDa. The values of [η] and r_h, have also been obtained for all the systems under study (see Table 1). The expected values for both hydrodynamic properties have been obtained for mAbs and g-eHER2 [9,12,18].

Table 1. Hydrodynamic and molecular properties of g-eHER2, mAbs and complexes present in the highest proportions, obtained from DLS, SEC and tetradetection.

Sample	M_w (kDa) s.d. < 2 %	[η] ($cm^3 \cdot g^{-1}$) s.d. ± 0.2	dA/dc ($mL g^{-1} cm^{-1}$) s.d. ±0.02	$D_s \times 10^7$ ($\mu m^2 \cdot s^{-1}$) s.d. ± 0.2	r_h (nm) s.d. ± 0.1
Trastuzumab - TZM	147.0	6.5	1.38 (1.40)	58.1	5.5
Pertuzumab - PZM	146.4	6.4	1.29 (1.36)	58.2	5.5
g-eHER2	86.4	6.5	0.90 (0.90)	44.6 *	4.7*
HER2/TZM	234.0	7.4*	n.d.	31.6*	6.8*
HER2/PZM/HER 2	320.0	8.6	n.d.	n.d.	7.4

*Obtained from refs. 9, 12 at T = 293 K. The values in parentheses have been calculated at 280 nm^{-1} using the protein Calculator v.3.4 tool.

We have extracted the experimental values of the absorption coefficient dA/dc from the UV detector, by matching the protein concentration with the value obtained from the refractive index (RI) detector. The values obtained for dA/dc for mAbs and g-eHER2 samples are listed in Table 1. Trastuzumab (1.38 ± 0.01 mL·g) shows a higher value of dA/dc than pertuzumab (1.29 ± 0.01 mL·g). The experimental variability is lower than 1 % among 5 independent measurements in each case. Both mAbs show a high degree of chemical similarity. There are subtle differences in the amounts of

Preprints (www.preprints.org) | NOT PEER-REVIEWED | Posted: 9 June 2023 doi:10.20944/preprints202306.0676.v1

tyrosine (Tyr), tryptophan (Trp) and phenylalanine (Phe) residues. These differences have an impact in the dA/dc measured by means UV spectroscopy. The extinction coefficient at 280 nm is unique for each protein, depending on the number of aromatic residues (Tyr, Trp and Phe), but it can also be affected by the solvent, the temperature and the pH. We have used the Protein Calculator Resource (http://protcalc.sourceforge.net/) to calculate dA/dc for the samples under study using the corresponding amino acid sequence. The extinction or absorption coefficients in water are estimated in this case using the method of Gill and von Hippel at 280 nm [19]. The results obtained match with the experiments.

In Figure 1 (down) the RI profiles obtained for the 1:3 antigen-antibody solutions are shown. The peaks appearing at the lowest retention volumes indicate the formation of complexes between both the g-eHER2 receptor and the mAbs. For the HER2/Trastuzumab mixture two peaks at retention volumes of 15.4 mL and 14.1 mL are clearly resolved, with molecular weights of 234 and 320 kDa, respectively. These values agree with the formation of both a heterodimer (HER2/trastuzumab or complex 1) and heterotrimer (HER2/trastuzumab/HER2 or complex 2). The deconvolution of the signals allows one to determine the total concentration, and the corresponding to both complexes 1 and 2. The data yield a proportion of $0.31C_T$ for complex 1 and $0.10C_T$ for complex 2, being C_T the total concentration of protein measured (Table 2). In the conditions used in this study, the highest proportion of complex obtained in this case corresponds to the heterodimer. In the case of HER2/pertuzumab mixture also two elution peaks are observed, located around very similar values of retention volumes to those obtained in HER2/trastuzumab mixture. However, the trend is reversed, since it is mostly obtained the heterotrimer (HER2/pertuzumab/HER2) in which the two fabs of the antibody bind to an antigen. In this case the concentrations are $012C_T$ for the heterodimer and $0.27C_T$ for the heterotrimer.

Table 2. Initial and equilibrium molar concentrations (μM) of the systems studied.

	Initial concentrations s.d. < 2 %		Equilibrium concentrations s.d. < 2 %			
Sample	**mAb**	**g-eHER2**	**Complex 1**	**Complex 2**	**Free mAb**	**Free g-eHER2**
HER2/TZM	4.78	1.46	1.12	0.26	3.37	0.08
HER2/PZM	4.76	1.16	0.42	0.68	3.36	0.04

From these results both the total concentration of antigen and antibodies and the equilibrium concentration of complexes and free antigen can be calculated, (Table 2). These data allow one to compare the binding affinity of these two antibodies with the g-eHER2 antigen in aqueous solutions at 309 K. The main question here relates to the antibody valence. Trastuzumab and pertuzumab molecules have two binding sites (Fab domains) able to interact with the g-eHER2. In fact, two different complexes are clearly observed in Figure 1 for both systems. In this specific case we may use the Goldberg's equation developed for bivalent antibodies [20,21].

$$K = \frac{f M_a p}{4c_a(1-p)\left(1-p\frac{f c_g M_a}{2 c_a M_g}\right)} \quad (3)$$

c_a and c_g are total antibody and antigen concentration in $g{\cdot}L^{-1}$, M_a and M_g are the molecular mass of antibody and antigen, f is the number of binding sites in the antiboby, and p the fraction of the reacted antigen sites that can be obtained from:

$$c_{ag} = c_g(1-p)^f \quad (4)$$

being c_{ag} the free antigen concentration in $g{\cdot}L^{-1}$. The higher the affinity of the antibody, the higher its equilibrium constant. This may be expressed by means of the equation:

$$-\ln K_a = \frac{\Delta G}{RT} \quad (5)$$

with ΔG the change in free energy, R is the universal gas constant (= 1.987 $cal{\cdot}K^{-1}{\cdot}mol^{-1}$) and T is the absolute temperature (309 K). To convert K_a to the SI units of energy, K_a must be expressed in [mole

Preprints (www.preprints.org) | NOT PEER-REVIEWED | Posted: 9 June 2023 doi:10.20944/preprints202306.0676.v1

fraction]$^{-1}$ rather than in units of M^{-1} [7]. The values obtained for ΔG from equation (4) are listed in Table 3.

Table 3. Equilibrium parameters and determination of the free energy, ΔG, of antigen-antibody interactions.

Sample	K_a (mole fraction^{-1})×10^{-7} s.d. < 2 %	ΔG (kcal·mol^{-1}) s.d. < 2 %
HER2/Trastuzumab	2.49	-10.4
HER2/Pertuzumab	3.17	-10.6

3.2. In-silico binding

In our study, we used the PRODIGY webserver to evaluate the different terms in equation (2) for each structure equilibrated through MD simulations. For each system, namely HER2/trastuzumab and HER2/pertuzumab, we uploaded 3 replicas containing 20 snapshots each. The estimated ΔG_{bind} values were then averaged over the last 20 snapshots for each system and are collected in Table 4. Further details regarding the different contributions accounted for the estimation of ΔG_{bind} can be found in the Supplementary Material section.

Based on the results shown in Table 4, the PRODIGY QSAR equation predicts that pertuzumab is a marginally better binder than trastuzumab. This finding is also supported by the crystallographic structures submitted to the PRODIGY protocol, which yielded lower ΔG_{bind} values for pertuzumab compared to trastuzumab (-10.3 kcal·mol^{-1} versus -12.0 kcal·mol^{-1}). Additionally, the pertuzumab complex exhibited a slightly larger number of ICs, which contributed the most to the QSAR equation (2).

Table 4. ΔG_{bind} values estimated at T = 309 K using the PRODIGY protocol. .

System	ΔG (kcal·mol^{-1})	
	Crystal Structures	MD Structures
HER2/Trastuzumab	-10.3	-11.0 ± 0.8
HER2/Pertuzumab	-12.0	-12.2 ± 0.9

Table 5 shows the number of ICs per property and the % of NIS percentage per property for the crystallographic structures, as well as the corresponding averages for the structures obtained by MD simulations. It is evident that the ICs involving charged-polar and ICs polar-polar interactions are quite similar in the HER2/trastuzumab and HER2/pertuzumab complexes. The most remarkable differences are found in the $ICs_{charged/apolar}$ and $ICs_{polar/apolar}$, which are larger in the HER2/pertuzumab case, giving rise to a more favorable binding energy. The NIS percentage contribution is, however, rather similar for both systems.

Table 5. Percentage of nature-dependent antigen-antibody interfacial contacts (ICs) and of non-interacting surface (NIS) calculated with the PRODIGY protocol on crystallographic structures and structures extracted from MD simulations (averaged values over 20 structures, see text for details). The number of ICs per property is also shown.

QSAR component	HER2/Trastuzumab		HER2/Pertuzumab	
	Crystal	MD	Crystal	MD
NIS charged (%)	21	20 ± 1	21	20 ± 1
NIS apolar (%)	36	38 ± 1	37	38 ± 1
Number of ICs per property				
ICs charged-charged	7	8 ± 4	3	3 ± 1
ICs charged-polar	7	12 ± 5	13	12 ± 2
ICs charged-apolar	16	20 ± 5	23	22 ± 4
ICs polar-polar	2	5 ± 3	10	6 ± 1

Preprints (www.preprints.org) | NOT PEER-REVIEWED | Posted: 9 June 2023 doi:10.20944/preprints202306.0676.v1

ICs polar-apolar	8	12 ± 3	24	20 ± 3
ICs apolar-apolar	21	29 ± 2	17	17 ± 4

4. Discussion

4.1. Binding Affinity

The experimental methodology employed in this study provides a reliable and unambiguous determination of antigen-antibody binding energies using complete mAbs in physiological aqueous solutions. The resulting experimental ΔG_{bind} values are in excellent agreement with the results obtained through the chosen "in-silico" approach. This consistency further confirms the outstanding performance of the QSAR model, which, in turn, was derived from carefully curated experimental data including some antigen-antibody complexes [11].

It is interesting to note the discriminatory ability of the $ICs_{charged/apolar}$ and $ICs_{polar/apolar}$ descriptors in the QSAR equation (2). In principle, it may seem counterintuitive that polar-apolar or charged-apolar interactions contribute to a decrease of ΔG_{bind} value. However, our observations in the antigen-antibody systems studied here reveal that the interaction between apolar and polar/charged aminoacids is a consequence of the close proximity of residues between antibody and antigen, as well as the arrangement of polar, apolar, and charged residues in each protein ternary structure. To illustrate this, Figure 2 displays the interaction between PHE257 residue of the extracellular HER2 domain and ILE58, TYR59 and GLN61 residues of the pertuzumab heavy chain Fab.

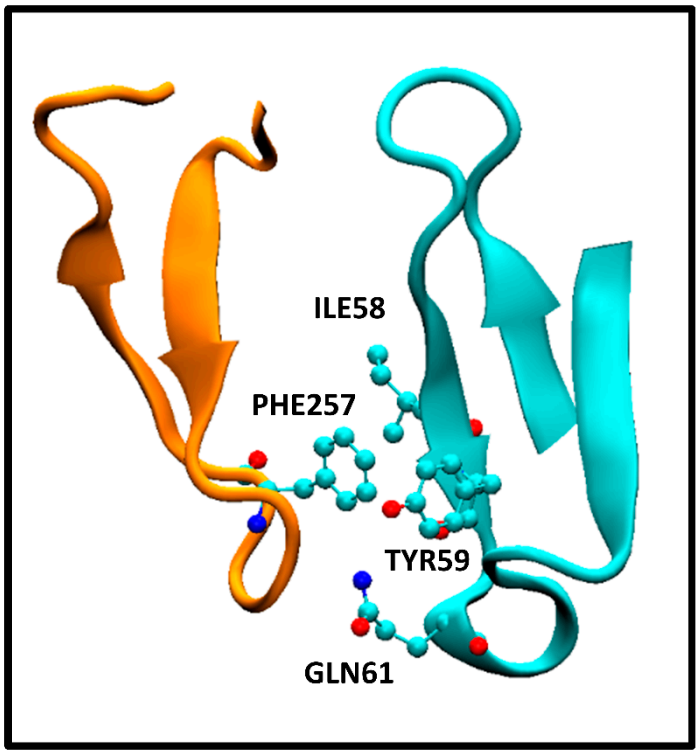

Figure 2. Interaction between EC HER2 PHE257 and pertuzumab Fab heavy chain variable domain ILE58, TYR59 and GLN61 residues. The specific amino acids are in a ball and stick representation. HER2 and pertuzumab Fab fragments as orange and cyan cartoon representations, respectively.

This correspond to the crystallographic structure of the HER2/pertuzumab complex (PDB Code: 1S78) analyzed using the PRODIGY protocol. In this structure, three contacts can be observed, namely, an apolar/polar interaction between one GLN61 and PHE257 and two apolar/apolar interactions between ILE58-TYR59 and PHE257. The former one contributes to $ICs_{polar/apolar}$ while the latter two interactions contribute to $ICs_{apolar/apolar}$. These interactions form part of a network of contacts

Preprints (www.preprints.org) | NOT PEER-REVIEWED | Posted: 9 June 2023 doi:10.20944/preprints202306.0676.v1

between aminoacids from both the antibody and antigen, resulting in a tightly bound complex. The presence of those polar/apolar and charged/apolar interactions correlates with this enhanced binding observed, as the PRODIGY QSAR equation. In contrast, the HER2/trastuzumab complex comprises a higher number of $ICs_{apolar/apolar}$ compared to the HER2/pertuzumab complex. However, these specific interactions have not been considered in the QSAR model, although they contribute to the Buried Surface Area (BSA). Consequently, the BSA values reported for the crystallographic structures indicate a larger value for the HER2/trastuzumab complex (1,350 Å^2) compared to HER2/pertuzumab complex (1,210 Å^2). Vangone et al. showed the superior performance of the model described in equation (2) compared to models that soley rely on BSA estimations [11].

4.2. Antigen-antibody complexes stoichiometry

In this work, we have experimentally shown that the IgG form of pertuzumab can bind two HER2 antigens, one per available Fab, more easily than trastuzumab (Figure 1). To provide a possible explanation of this observation, we have built purely geometric models for the complete IgG form of the antibodies with two molecules of the extracellular HER2 domain bound to each Fab fragment.

Figure 3 illustrates the arrangement of both HER2 extracellular domains bound to the two antibody Fabs. It is evident that trastuzumab may experience more steric hindrance than pertuzumab when accommodating two HER2 antigens on the same IgG antibody. This observation can account for the preferential 2:1 stoichiometry observed in the pertuzumab complex. A similar explanation was given for IgM antibody forms by Samsudin et al. [22].

It is worth noting that we previously studied the structure of the trastuzumab antibody bound to one and two HER2 extracellular domains [9,12]. In these works we analyzed its hydrodynamic properties were analyzed. Upon revisiting the simulated systems and examining any potential interferences between both HER2 proteins in the 2:1 complex, we have not found any significant steric hindrance between both HER2 proteins.

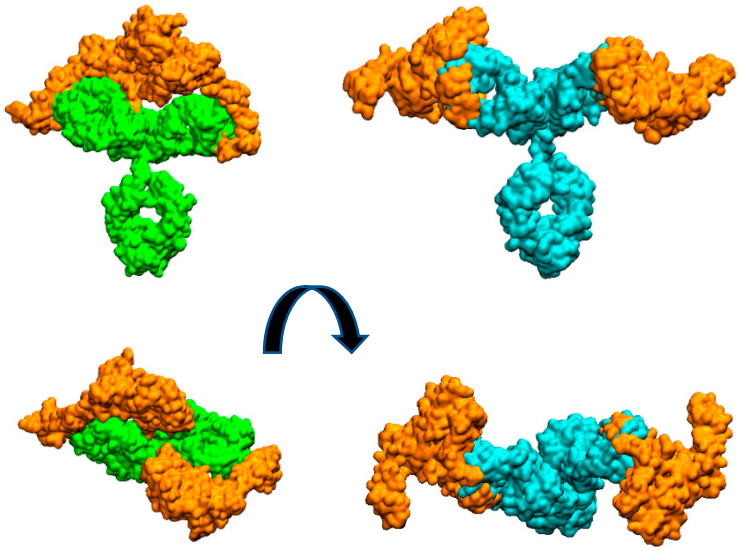

Figure 3. Molecular surfaces showing the relative disposition of whole Mabs with two HER2 extracellular domain proteins (orange colour) bound to each Fab. Pertuzumab is colored cyan and trastuzumab is colored green. Figures at bottom are perpendicular views of the upper ones.

It can be illustrative to consider the sequential binding of a second HER2 unit to a HER2/trastuzumab complex, where a first HER2 protein has already bound. In the present work, we used those simulations to explore whether the mobility of the HER2-trastuzumab Fab bound complex, relative to the unbound Fab within the IgG molecule, could potentially hinder the binding of a second HER2 protein. Video 1 in the Supplementary Material section shows a recording from a MD simulation, demonstrating the flexibility of the Fab arms in the IgG structure when one of them

Preprints (www.preprints.org) | NOT PEER-REVIEWED | Posted: 9 June 2023 doi:10.20944/preprints202306.0676.v1

is bound to an HER2 protein. Taking this flexibility into consideration, we sequentially fitted another HER2 protein in the available Fab. This was repeated for several structures of the 1:1 complex obtained from the MD simulations performed in our previous work. For the fitting procedure, we use the substructure formed by the bound HER2 and the Fab light chain. That set was superimposed on the light chain of the available Fab resulting in a virtual 2:1 complex. The result can be visualized in Figure 4.

The resulting root mean square distance (RMSD) between the backbone atoms of the two light chain fragments was around 2 Å. The observed collapse between the two HER2 substructures is clearly evident, enhancedby the interpenetration of their surfaces. Although this analysis is a rigid procedure showed for illustrative purposes, it can effectively convey the difficulties associated with the binding of a second HER2 protein to the HER2/trastuzumab 1:1 complex to form the 2:1 antigen/antibody configuration.

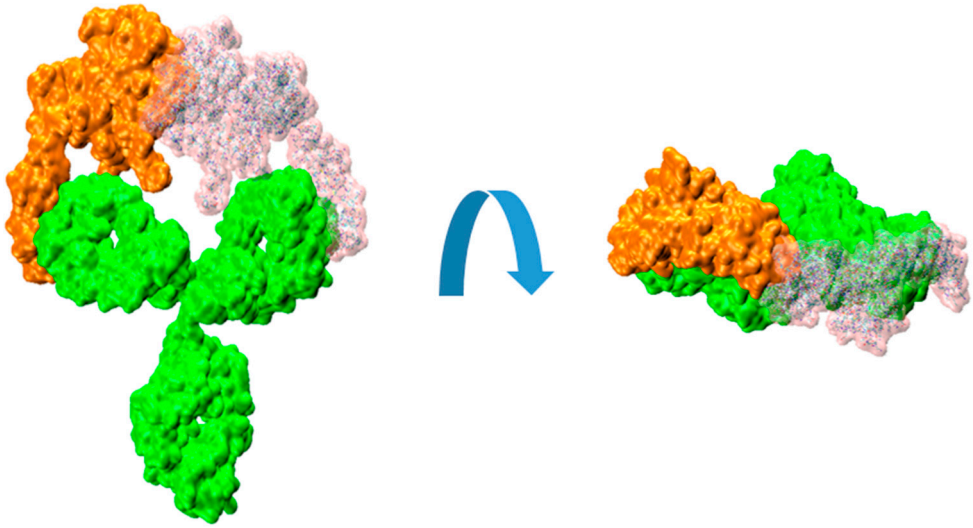

Figure 4. Molecular surfaces showing the relative disposition of Trastuzumab IgG (green colour) with a bound HER2 extracellular domain proteins (orange colour) and another HER2 (transparent pink colour) fitted on the available Fab, as described in the text.

5. Conclusions

In this study a combined experimental and in-silico analysis was conducted to investigate the binding process of trastuzumab and pertuzumab mAbs to the extracellular HER2 domain. The experimental setup employed size exclusion chromatography to separate protein complexes by size, enabling the determination of ΔG_{bind} by the differentiation between different stoichiometries and the determination of the concentration of each species. The binding free energy obtained from this label-free experimental methodology experiments is in excellent agreement with in-silico results, showing that pertuzumab is a marginally better binder than trastuzumab. At this respect, the QSAR model PRODIGY employed in the "in-silico" analysis revealed that the pertuzumab complex presents more interfacial contacts (ICs) than the trastuzumab complex. More specifically, the pertuzumab complex presents a higher number of ICs of the charged/apolar and polar/apolar types, which significantly contribute to reduce the ΔG_{bind} in the QSAR model. These favorable contacts observed can be attributed to the local approximations of charged or polar residues to apolar aminoacids, constituting an enhanced interaction network. Furthermore, the study reveals two types of associations can for these antibodies, namely, the intrinsic association (affinity) for the monovalent interaction and functional affinity (avidity) for the divalent interaction. The antibody IgG forms used in the experiments showed a superior avidity, the preferential divalent functionality, of pertuzumab over trastuzumab. This preference may reside in the close proximity between both antigens bound to the two available Fab arms of the IgG trastuzumab antibody. It should be highlighted that the results of this study are obtained from unmodified and label-free mAbs in solution, which offers interesting

advantages. Firstly, it avoids any possible alteration of the mAbs structure or function that may occur during modification or labeling. Secondly, it minimizes the risk of interference of the modifications in the interaction between the mAbs and HER2. Additionally, the use of unmodified and label-free mAbs allows experiments to be performed under physiological conditions, better reflecting the conditions under which interactions occur in the human body.

Supplementary material: 1. Word file containing part of the PRODIGY binding energy calculation results showing the number of intermolecular contacts and residue-residue interactions for a particular MD frame structure of the HER2-trastuzumab complex. 2. Word file containing part of the PRODIGY binding energy calculation results showing the number of intermolecular contacts and residue-residue interactions for a particular MD frame structure of the HER2-pertuzumab complex. 3. GIF Video illustrating the flexibility of the extracellular-HER2-trastuzumab complex.

Author Contribution: "Conceptualization, J.F.V., V.L.C. and J.C.; Methodology, J.F.V., V.S., J.R. and V.L.C.; Software, J.R.; Validation, J.C., M.G. and J.P.; Formal Analysis, J.R.; Investigation, J.F.V., V.S., J.R. and V.L.C.; Resources, J.C., M.G. and J.P.; Writing – Original Draft Preparation, J.F.V. and V.C.; Writing – Review & Editing, all authors; Visualization, all authors; Supervision, J.C.; Funding Acquisition, J.F.V and J.R.

Funding and Acknowledgments: This research work was funded by the Fundación FERO and Fundación "Contigo contra el cancer de la mujer". J.R. acknowledges funding from the Project "Bioinformatic study of the interactions between membrane proteins associated to breast cancer and antibodies", PIE202050E017 (CSIC). The authors also gratefully acknowledge to the SGAI-CSIC for its assistance and help while using of the DRAGO Supercomputer.

Conflict of Interest: The authors report there are no competing interests to declare

References

1. Cesca, M. G.; Vian, L.; Cristóvão-Ferreira, S.; Pondé, N.; de Azambuja, E. HER2-Positive Advanced Breast Cancer Treatment in 2020. *Cancer Treat. Rev.* **2020**, *88* (April). https://doi.org/10.1016/j.ctrv.2020.102033.
2. Cho, H. S.; Mason, K.; Ramyar, K. X.; Stanley, A. M.; Gabelli, S. B.; Denney, D. W.; Leahy, D. J. Structure of the Extracellular Region of HER2 Alone and in Complex with the Herceptin Fab. *Nature* **2003**, *421* (6924), 756–760. https://doi.org/10.1038/nature01392.
3. Franklin, M. C.; Carey, K. D.; Vajdos, F. F.; Leahy, D. J.; de Vos, A. M.; Sliwkowski, M. X. Insights into ErbB Signaling from the Structure of the ErbB2-Pertuzumab Complex. *Cancer Cell* **2004**, *5* (4), 317–328. https://doi.org/10.1016/s1535-6108(04)00083-2.
4. Troise, F.; Cafaro, V.; Giancola, C.; D'Alessio, G.; De Lorenzo, C. Differential Binding of Human Immunoagents and Herceptin to the ErbB2 Receptor. *FEBS J.* **2008**, *275* (20), 4967–4979. https://doi.org/10.1111/j.1742-4658.2008.06625.x.
5. Lua, W. H.; Gan, S. K. E.; Lane, D. P.; Verma, C. S. A Search for Synergy in the Binding Kinetics of Trastuzumab and Pertuzumab Whole and F(Ab) to Her2. *npj Breast Cancer* **2015**, *1*. https://doi.org/10.1038/npjbcancer.2015.12.
6. Spiegelberg, D.; Stenberg, J.; Richalet, P.; Vanhove, M. K D Determination from Time-Resolved Experiments on Live Cells with LigandTracer and Reconciliation with End-Point Flow Cytometry Measurements. *Eur. Biophys. J.* **2021**, *50* (7), 979–991. https://doi.org/10.1007/s00249-021-01560-2.
7. Hao, Y.; Yu, X.; Bai, Y.; McBride, H. J.; Huang, X. Cryo-EM Structure of HER2-Trastuzumab-Pertuzumab Complex. *PLoS One* **2019**, *14* (5). https://doi.org/10.1371/journal.pone.0216095.
8. Fuentes, G.; Scaltriti, M.; Baselga, J.; Verma, C. S. Synergy between Trastuzumab and Pertuzumab for Human Epidermal Growth Factor 2 (Her2) from Colocalization: An in Silico Based Mechanism. *Breast Cancer Res.* **2011**, *13* (3). https://doi.org/10.1186/bcr2888.
9. Vega, J. F.; Ramos, J.; Cruz, V. L.; Vicente-Alique, E.; Sanchez-Sanchez, E.; Sanchez-Fernandez, A.; Wang, Y.; Hu, P.; Cortes, J.; Martinez-Salazar, J. Molecular and Hydrodynamic Properties of Human Epidermal Growth Factor Receptor HER2 Extracellular Domain and Its Homodimer: Experiments and Multi-Scale Simulations. *Biochim. Biophys. Acta-General Subj.* **2017**, *1861* (9), 2406–2416. https://doi.org/10.1016/j.bbagen.2017.06.012.
10. Oda, M.; Uchiyama, S.; Noda, M.; Nishi, Y.; Koga, M.; Mayanagi, K.; Robinson, C. V.; Fukui, K.; Kobayashi, Y.; Morikawa, K.; Azuma, T. Effects of Antibody Affinity and Antigen Valence on Molecular Forms of Immune Complexes. *Mol. Immunol.* **2009**, *47* (2–3), 357–364. https://doi.org/10.1016/j.molimm.2009.09.009.
11. Vangone, A.; Bonvin, A. M. J. J. Contacts-Based Prediction of Binding Affinity in Protein–Protein Complexes. *Elife* **2015**, *4* (JULY2015), 1–15. https://doi.org/10.7554/eLife.07454.

12. Ramos, J.; Vega, J. F.; Cruz, V.; Sanchez-Sanchez, E.; Cortes, J.; Martinez-Salazar, J. Hydrodynamic and Electrophoretic Properties of Trastuzumab/HER2 Extracellular Domain Complexes as Revealed by Experimental Techniques and Computational Simulations. *Int. J. Mol. Sci.* **2019**, *20* (5). https://doi.org/10.3390/ijms20051076.
13. Corp., D. S. B. Discovery Studio 2022. 2022.
14. Maier, J. A.; Martinez, C.; Kasavajhala, K.; Wickstrom, L.; Hauser, K. E.; Simmerling, C. Ff14SB: Improving the Accuracy of Protein Side Chain and Backbone Parameters from Ff99SB. *J. Chem. Theory Comput.* **2015**, *11* (8), 3696–3713. https://doi.org/10.1021/acs.jctc.5b00255.
15. Case Ross C Walker, D. A.; Darden Junmei Wang, T. Amber 2016 Reference Manual Principal Contributors to the Current Codes.
16. Xue, L. C.; Rodrigues, J. P.; Kastritis, P. L.; Bonvin, A. M.; Vangone, A. PRODIGY: A Web Server for Predicting the Binding Affinity of Protein-Protein Complexes. *Bioinformatics* **2016**, *32* (23), 3676–3678. https://doi.org/10.1093/bioinformatics/btw514.
17. Kastritis, P. L.; Rodrigues, J. P. G. L. M.; Folkers, G. E.; Boelens, R.; Bonvin, A. M. J. J. Proteins Feel More than They See: Fine-Tuning of Binding Affinity by Properties of the Non-Interacting Surface. *J. Mol. Biol.* **2014**, *426* (14), 2632–2652. https://doi.org/10.1016/j.jmb.2014.04.017.
18. Vicente-Alique, E.; Núñez-Ramírez, R.; Vega, J. F.; Hu, P.; Martínez-Salazar, J. Size and Conformational Features of ErbB2 and ErbB3 Receptors: A TEM and DLS Comparative Study. *Eur. Biophys. J.* **2011**, *40* (7), 835–842. https://doi.org/10.1007/s00249-011-0699-y.
19. Gill, S. C.; von Hippel, P. H. Calculation of Protein Extinction Coefficients from Amino Acid Sequence Data [Published Erratum Appears in Anal Biochem 1990 Sep;189(2):283]. *Anal Biochem* **1989**, *182* (2), 319–326.
20. Goldberg, R. J. A Theory of Antibody-Antigen Reactions. II. Theory for Reactions of Multivalent Antigen with Multivalent Antibody. *J. Am. Chem. Soc.* **1953**, *75* (13), 3127–3131. https://doi.org/10.1021/ja01109a025.
21. Karagiannis, P.; Singer, J.; Hunt, J.; Gan, S. K. E.; Rudman, S. M.; Mechtcheriakova, D.; Knittelfelder, R.; Daniels, T. R.; Hobson, P. S.; Beavil, A. J.; Spicer, J.; Nestle, F. O.; Penichet, M. L.; Gould, H. J.; Jensen-Jarolim, E.; Karagiannis, S. N. Characterisation of an Engineered Trastuzumab IgE Antibody and Effector Cell Mechanisms Targeting HER2/Neu-Positive Tumour Cells. *Cancer Immunol. Immunother.* **2009**, *58* (6), 915–930. https://doi.org/10.1007/s00262-008-0607-1.
22. Samsudin, F.; Yeo, J. Y.; Gan, S. K. E.; Bond, P. J. Not All Therapeutic Antibody Isotypes Are Equal: The Case of IgM: Versus IgG in Pertuzumab and Trastuzumab. *Chem. Sci.* **2020**, *11* (10), 2843–2854. https://doi.org/10.1039/c9sc04722k.